Journal of Physics and Chemistry of Solids 96-97 (2016) 121–127

Contents lists available at ScienceDirect

Journal of Physics and Chemistry of Solids

journal homepage: www.elsevier.com/locate/jpcs

A first-principle study of Os-based compounds: Electronic structure and vibrational properties

N. Arıkan [a,*], O. Örnek [b], Z. Charifi [c], H. Baaziz [c], Ş. Uğur [d], G. Uğur [d]

[a] Science Education Department, Education Faculty, Ahi Evran University, 40100 Kırşehir, Turkey
[b] Department of Materials and Metallurgical Engineering, Ahi Evran University, Kırşehir 40200, Turkey
[c] Physics department, Faculty of Science, University of M'sila, 28000 M'sila, Algeria
[d] Department of Physics, Faculty of Science, Gazi University, 06500 Ankara, Turkey

ARTICLE INFO

Article history:
Received 11 September 2015
Received in revised form
1 April 2016
Accepted 16 May 2016
Available online 17 May 2016

Keywords:
DFT
Elastic constants
Ductility
İntermetallic alloys
Specific heat capacity

ABSTRACT

The electronic structure, elastic, and phonon properties of OsM (M=Hf, Ti, Y and Zr) compounds are studied using first-principles calculations. Elastic constants of OsY and specific heat capacity of OsM (M=Hf, Ti, Y, and Zr) are reported for the first time. The predicted equilibrium lattice constants are in excellent agreement with experiment. The calculated values of bulk moduli are considerably high but are much smaller than that of Osmium, which is around 400 GPa. The phase stability of the OsM (M=Hf, Ti, Y and Zr) compounds were studied by DOS calculations and the results suggest that OsY is unstable in the B2 phase. The brittleness and ductility properties of OsM (M=Hf, Ti, Y and Zr) are determined. OsM (M=Hf, Ti, Y and Zr) compounds are predicted to be ductile materials. The electronic structure and phonon frequency curves of OsM (M=Hf, Ti, Y and Zr) compounds are obtained. The position of Fermi level of these systems was calculated and discussed in terms of the pseudo gaps. The finite and small DOS at the Fermi level 0.335, 0.375, 1.063, and 0.383 electrons/eV for OsHf, OsTi, OsY, and OsZr, respectively, suggest that OsM (M=Hf, Ti, Y and Zr) compounds are weak metals.

1. Introduction

Intermetallic compounds are of interest because of their oxidation resistance, high melting point, strength at high temperatures, superconducting properties [1,2], hydrogen storage capability [3,4], and medical applications [5]. Recently, considerable effort has been directed towards the understanding of structural stabilities and the phase diagrams of the transition metals and compounds formed by Group IV elements T (T=Ti, Zr, Hf) and platinum group elements M (M=Ru, Rh, Pd, Os, Ir, Pt) [6,7].

At high temperature, the Os–Ti and Hf–Os alloys have been studied by direct reaction calorimetry. The formation enthalpies of the intermetallic compounds HfOs and OsTi were measured [6]. The formation enthalpies and structural phase stabilities of several binary transition-metals with the chemical formula XY and XY_3 compounds formed by X (X=Ti, Zr, Hf) and platinum group elements Y (Y=Ru, Rh, Pd, Os, Ir, Pt) were estimated using the first-principles local density functional (LDA) approach [7]. The complete phase diagram of the Zr–Os alloy was established by Eremenko et al. [8] and the alloys containing a small amount of osmium were studied [9]. The microstructure and phase composition of the quenched and aged Zr–Os alloys containing 0.25 to 5 at% of osmium were investigated [10]. A decomposition of the β-phase (centered cubic phase) into the α-phase (hexagonal phase) and a β-phase enriched with osmium occur during quenching in the Zr–0.25 at% Os and Zr–0.5 at% Os alloys. The X-ray diffraction patterns of the Zr–0.25 at% Os alloy contain only the α-phase lines. α-phase lattice parameters in this alloy are about $a=0.3232$ nm, $c=0.5148$ nm, $c/a=1.594$,which coincide with the lattice parameters of the α-phase alloys of pure zirconium. In addition, in the Zr–5 at% Os alloy, only the β-phase is observed by X-ray diffraction analysis with a lattice parameter $a=0.3558$ nm.

The OsTM and $TMOs_2$ compounds have been reported to show no super-hard character, but they behave like ductile materials [11]. The formation enthalpies of 4*d* and 5*d* transition metals have been measured by high-temperature direct synthesis calorimetry at 1373 K. They have been compared with the predicted data of Miedema et al. and with those found by *ab initio* calculations [12]. A thermodynamic study of experimental thermochemical and phase diagram data of the Hf–Os alloy was performed employing the CALculation of PHAse Diagrams (CALPHAD) method, and different thermodynamic parameters of the Hf–Os alloys were

* Corresponding author.
E-mail addresses: nihat.arikan@hotmail.com (N. Arıkan), charifizoulikha@gmail.com (Z. Charifi).

http://dx.doi.org/10.1016/j.jpcs.2016.05.009
0022-3697/

obtained [13].

In order to understand the physical properties and chemical behaviors of the intermetallic compounds for technological applications, a complete investigation of relevant alloy systems is important. In the present work, we focus on investigating the physical properties of Os-based compounds OsM (M=Hf, Ti, Y and Zr), such as elastic constants, band structures, and vibrational properties by the plane-wave pseudopotential density functional theory method through the Quantum ESPRESSO code [14], and also constant-volume specific heat capacity was calculated by the quasi-harmonic approximation (QHA) [15]. We focus especially on the investigation of the stability of OsY in the B2 phase.

This paper is organized as follows. The description of our calculation methods is presented in Section 2. The structural and vibrational properties of OsM (M=Hf, Ti, Y and Zr) compounds are discussed in Section 3, including the comparison with experiment. In Section 3, the electronic structure of these compounds is also investigated. Conclusion is given in Section 4.

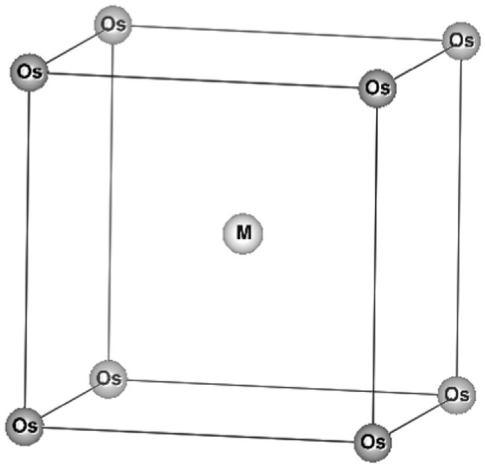

Fig. 1. Crystal structure of OsM (M=Hf, Ti, Y and Zr) in the B2 phase. OsM unit cell contains two atoms, Os and M, one occupies the position 1a (0,0,0) and the other the position 1b (0.5,0.5,0.5).

2. Method of calculation

2.1. Total energy electronic structure calculations

Many intermetallics with the approximate composition AB crystallize in the B2 structure, which is also known as the CsCl structure (see Fig. 1). In the completely ordered state, A atoms occupy one cubic primitive sublattice and B atoms occupy the rest. This means that each A atom is surrounded by eight B atoms in the nearest neighbor sites, and vice versa. The binary compounds OsM (M=Hf, Ti, Y and Zr) were observed to have the cubic B2 structure [6,10,16,17], which was confirmed by *ab initio* calculations given in Ref. [2]. The structure of OsY was not identified experimentally but it was reported to be B2 phase with a formation energy equals to 0.021 eV/atom [18]. The formation energies were calculated at $T=0$ and $P=0$ for different structures: $L1_1$, B1, B2, B3, and B_h.

The formation enthalpies of OsZr, OsHf, and OsTi are found to be all negative. This is an indication of the stability of these compounds in the B2 structure [6]. The calculations of the total energies were performed with the Quantum ESPRESSO (QE) code [14]. The exchange-correlation potential was treated with the generalized gradient approximation of Perdew–Burke–Ernzerhof (PBE-GGA) [19]. Ultrasoft pseudopotentials from the Quantum Espresso library are used for most elements, including Ti, Y, Zr, and Os. Publicly available pseudopotentials are used for the OsHf compound, including ultrasoft Os and Hf pseudopotentials created by the Rappe group [20]. The energies were calculated at zero temperature and pressure. The accuracy of the first-principles calculations depends on the choice of convergence conditions, such as forces and stress tensors and the sets of special **k**-points. In our calculations, the scheme of Monkhorst and Pack [21] was used for the Brillouin zone **k**-point sampling. The energy cutoff for the expansion of the eigenfunctions was set to 40 Ry. To evaluate the electronic charge density, the kinetic energy cutoff was set to 400 Ry. The irreducible wedge of the first Brillouin zone was sampled using 1000 **k**-points. Integration up to the Fermi surface was performed using the Methfessel–Paxton smearing technique [22] with a smearing parameter of $\sigma=0.02$ Ry. With these choices, the total energy was converged to 10^{-5} Ry and the maximum force allowed on each atom was 0.002 Ry/a.u. Having obtained self-consistent solutions of the Kohn–Sham equations, the lattice-dynamical properties were calculated within the framework of the self-consistent density functional perturbation theory [23]. To obtain the complete phonon dispersions and density of states, eight dynamical matrices were calculated on a $(4\times4\times4)$ **q**-point mesh. These dynamical matrices were calculated using the Fourier deconvolution on this mesh. The ground state of OsM (M=Hf, Ti, Y and Zr) compounds was obtained by optimizing the total energy as function of the lattice parameters.

2.2. Elastic constants calculations

The elastic constants of a material describe its response to an applied stress or, conversely, the stress required to maintain a given deformation, and can be used to evaluate the elastic properties. These properties are related directly to mechanical stability. The elastic constants provide an estimation of the melting temperature and the strength [24].

The calculated elastic parameters are obtained from the energy variation $\frac{\Delta E}{V}$ described in Ref. [25].

For the strain under hydrostatic pressure $\boldsymbol{e}=(\delta, \delta, \delta, 0, 0, 0)$, the total energy change is transformed to:

$$\frac{\Delta \boldsymbol{E}}{\boldsymbol{V}}=\frac{9}{2}\boldsymbol{B}\delta^2, \tag{1}$$

where B is the bulk modulus and given by the following equation:

$$B=(C_{11}+\mathbf{2}C_{12})/\mathbf{3}. \tag{2}$$

By applying the volume-conserving monoclinic strain $\boldsymbol{e}=(0, 0, \delta^2/(4-\delta^2), 0, 0, \delta)$, the total energy variation is given by the following formula:

$$\frac{\Delta \boldsymbol{E}}{\boldsymbol{V}}=\frac{1}{2}\boldsymbol{C}_{44}\delta^2+\boldsymbol{O}(\delta^4). \tag{3}$$

In the final step, we used the volume-conserving rhombohedral strain tensor given by $\boldsymbol{e}=(0, 0, (1+\delta)^{-2}-1, 0, 0, \delta)$, which transforms the total energy to

$$\frac{\Delta \boldsymbol{E}}{\boldsymbol{V}}=6\boldsymbol{C}'\delta^2+\boldsymbol{O}(\delta^3), \tag{4}$$

where C' is defined by $\boldsymbol{C}'=(\boldsymbol{C}_{11}-\boldsymbol{C}_{12})/2$.

Several sets of $\frac{\Delta E}{V}$ were calculated by varying δ in steps of 0.002. These data were fitted by a quadratic polynomial, and then the elastic constant is obtained from Eqs. (1)–(4).

Shear modulus (G) is derived using the following relation:

$$\boldsymbol{G}=\frac{\boldsymbol{C}_{11}-\boldsymbol{C}_{12}+3\boldsymbol{C}_{44}}{5}. \tag{5}$$

2.3. Constant-volume specific heat capacity calculations

Some thermodynamic properties such as the temperature dependence of entropy $S(T)$, constant-volume specific heat $C_V(T)$, and Helmholtz's free energy $F(T)$ can be effectively computed within a harmonic description of the lattice potential. Others (such as the thermal expansion $\alpha(T)$, the constant-pressure specific heat, $C_P(T)$, the temperature dependence of the bulk modulus, $B(T)$, the simultaneous dependence on temperature and pressure of entropy, $S(P,T)$, and Helmholtz's free energy, $F(P,T)$ require to go somehow beyond the harmonic approximation (HA). In this respect, the QHA provides the simplest formal frame allowing for their calculation by introducing an explicit dependence on volume of phonon frequencies and retaining the harmonic expression for the Helmholtz free energy [26].

The QHA is a very effective approach to study the thermodynamics of solids at low temperatures, but not at high temperatures where phonon–phonon interactions, or anharmonic effects, are important. This approximation treats phonons as if they did not interact as a phonon "gas". The system becomes equivalent to a collection of independent harmonic oscillators.

In the QHA, the Helmholtz free energy is given by

$$\boldsymbol{F(V,T)=E_{tot}(V)+F_{vib}(V,T)} \tag{6}$$

where first and second terms are the static energy of a crystal at a given volume and vibrational contributions, respectively. $\boldsymbol{F_{vib}(V,T)}$ is written in the following form:

$$\boldsymbol{F_{vib}(V,T)=k_BT\int g(\omega)\ln\left[2\sinh\left(\frac{\hbar\omega}{2k_BT}\right)\right]d\omega} \tag{7}$$

where $\boldsymbol{g(\omega)}$ is the phonon density of states. The heat capacity at constant volume $\boldsymbol{C_V^{vib}}$, is defined as

$$\boldsymbol{C_V^{vib}=-T\left(\frac{\delta^2F_{vib}(V,T)}{\delta T^2}\right)_V} \tag{8}$$

The constant-volume specific heat, $\boldsymbol{C_V^{vib}}(T)$ is calculated within the Harmonic approximation (HA) using QHA code for these compounds [15].

3. Results and discussion

3.1. Determination of the ground state parameters, elastic properties, and mechanical stability

A detailed study of the properties of Os-based compounds is required for further understanding of their stability. We optimized the structures of all compounds OsM (M=Hf, Ti, Y and Zr) by calculating the total energy versus volume, and then fitted the results with the Murnaghan equation of state [27]. The calculated lattice constant parameters for each compound using GGA approximation in B2 structure are listed in Table 1 and compared with the available experimental and theoretical data. Calculated data are in excellent agreement with experiments and previous theoretical works [7,11,18,28,29].

The calculated lattice parameters of OsM (M=Hf, Ti, Y and Zr) compounds are found to be in good agreement with the available experimental ones [28,29] with typical deviations of about 0.4% for OsTi, 0.49 % for OsZr, and 0.55% for OsHf.

The bulk modulus describes the elastic properties of a solid when it is under pressure on all surfaces. It is also defined as a measure of the ability of a substance to withstand changes in volume when under compression on all sides. The values of bulk moduli calculated using Eq. (1) are considerably high but much smaller than that of Osmium, which is around 400 GPa [30,31]. There is a good agreement between our bulk moduli and theoretical data [11] for OsHf, OsTi, and OsZr. One can note that the lattice parameter decreases when we move from OsHf to OsTi, and from OsY to OsZr. On the other hand, the bulk modulus increases as we go from OsHf to OsTi, and from OsY to OsZr. We note that the bulk modulus of OsTi is the largest one (248.86 GPa), so it is predicted to be the hardest in the investigated series.

Elasticity is a fundamental property of materials. The elastic constants of a single crystal are of interest because of the information they give about the nature of the binding forces in solids. In cubic materials, only three independent elastic constants C_{11}, C_{12} and C_{44}, are needed. The elastic constants of these cubic systems are obtained from Eqs. (1)–(4), which are described in detail elsewhere [25].

Table 1 shows the elastic constants obtained from our calculations and the results are compared with the literature values [11]. Our results are in close agreement with those calculated with the same method implemented in the Castep simulation package [11], except for C_{11} of OsHf and OsZr. Unfortunately, the experimental elastic constants for OsM (M=Hf, Ti, Y and Zr) are not available in the literature. Thus, further experimental studies are needed to compare with these computed results for the studied materials.

In general, all three fundamental elastic constants, C_{11}, C_{12} and C_{44}, are larger than those of Ref. [11]. The relative error of our calculated elastic constants compared to theoretical data reported by Liu [11] are between 0.9% and 10% for OsHf, 0.1% and 5% for OsTi, and 3% and 12% for OsZr.

Table 1
Calculated lattice constant a, bulk modulus B, and its pressure derivative B', elastic constants C_{ij} (GPa), shear modulus G (GPa), and B/G for OsM (M=Hf, Ti, Y and Zr) materials, compared with the available experimental and theoretical data.

Compounds		a (Å)	B	B'	C_{11}	C_{12}	C_{44}	G	B/G
OsHf	This work	3.257	224.43	4.26	393.69	139.79	110.05	116.81	1.92
	GGA [11]	3.294	223.7		366.1	152.6	105.6	106.1	2.10
	VASP [7]	3.251							
	Exp. [28]	3.239							
OsTi	This work	3.093	248.86	3.92	447.15	149.71	112.58	127.04	1.96
	GGA [11]	3.093	246.7		447.6	146.3	118.7	130.6	1.88
	VASP [7]	3.088							
	Exp. [28]	3.07							
	Exp. [29]	3.08							
OsY	This work	3.419	128.40	3.35	189.93	97.64	49.62	48.23	2.662
	Theory [18]	3.414							
OsZr	This work	3.279	210.881	3.26	383.074	124.784	90.421	105.911	1.991
	GGA [11]	3.282	206.5		341.4	139	87.7	92.9	2.22
	VASP [7]	3.331							
	Exp. [28]	3.263							

The mechanical stability of OsM (M=Hf, Ti, Y and Zr) compounds has been investigated theoretically using the following criteria [32]:

$$C_{44}>0,(C_{11}-C_{12})/2>0 \text{ and } B=(C_{11}+2C_{12})/3>0 \quad (9)$$

In Table 1, we see that these criteria are verified, suggesting that OsM (M=Hf, Ti, Y and Zr) compounds are mechanically stable in this structure.

The bulk modulus B and shear modulus G of OsM (M=Hf, Ti, Y and Zr) are calculated and presented in Table 1. For comparison, the values of those reported in [11] are presented. Generally speaking, one can see good agreement with the reported data for OsTi and OsZr compounds.

Brittleness and ductility properties of OsM (M=Hf, Ti, Y and Zr) compounds have also been studied using the shear modulus to bulk modulus B/G ratio. According to Pugh [33], if B/G ratio is smaller than 1.75, the material behaves in a brittle manner, otherwise the material behaves in a ductile manner. Our estimated values of B/G are given in Table 1, which show that the materials under study are all ductile compounds. In general, calculated results are found to be in good agreement with the results found by Liu et al. [11]. The little difference regarding the value of the ratio of Pugh is because Liu et al. used the Voigt–Reuss–Hill approximation, which is different from that applied in the present work in the calculation of this parameter. The Pugh ratio of B/G of OsHf was found to be lowest, which was followed by OsTi, OsZr, and OsY in an increasing order, indicating an increasingly ductile behavior.

3.2. Electronic and vibrational properties

The self-consistent scalar relativistic band structures of OsM (M=Hf, Ti, Y and Zr) compounds along the representative symmetrical directions of the Brillouin zone were obtained at the equilibrium volume within the GGA approximation. The Fermi level E_F is shown by a dashed horizontal line. All compounds exhibit a metallic behavior as shown in Fig. 2 where one can notice that the energy bands cross the Fermi level. It is clearly seen that they present a similar feature. All the Os-based compounds are weak metals as seen from the finite and small DOS at the Fermi level 0.335, 0.375, 1.063, and 0.383 states/eV-CELL for OsHf, OsTi, OsY and OsZr, respectively. Therefore, the OsHf shows a low metallicity and the highest hardness (224.43) compared to that of the OsY compound.

The total and partial density of states of OsM (M=Hf, Ti, Y and Zr) compounds are shown in Fig. 3. In these four compounds, there are pronounced pseudogaps near the Fermi level, orbital-projected DOS indicates strong hybridization of Os-*d* and M-*d* valence states below and on the Fermi energy.

With a total of 11 valence electrons in the unit cell, OsY fills its first three bands completely, the fourth and fifth bands nearly full, and leaves the sixth band slightly over half-filled. The Fermi level falls within the bonding states (Fig. 3c) for OsY and electron structure analysis reveals the mechanism for its instability in the B2 phase: the bonding states are only partially filled and the DOS at the Fermi level is high (1.063 states/eV-CELL).

The same behavior is observed in previous works on CoBe [34], FeAl [35], and ZrCr [36]. OsHf, OsTi, and OsZr , in contrast, pushes the Fermi level towards the antibonding peak and it is located in the “pseudo gap” which separates the bonding and antibonding states, and touches the very bottom of the seventh band near (Fig. 3a, b and d). The Fermi level lies in the region with the low density of the nonbonding states. All bonding states are thus fully occupied, and their density greatly exceeds the density of the nonbonding states. The bands in OsM (M=Hf, Ti, Y and Zr) compounds are dominated by a hybridization of Os *d*-states with M *d*-states under the Fermi level and above it. This is an indication of the covalent bonding character.

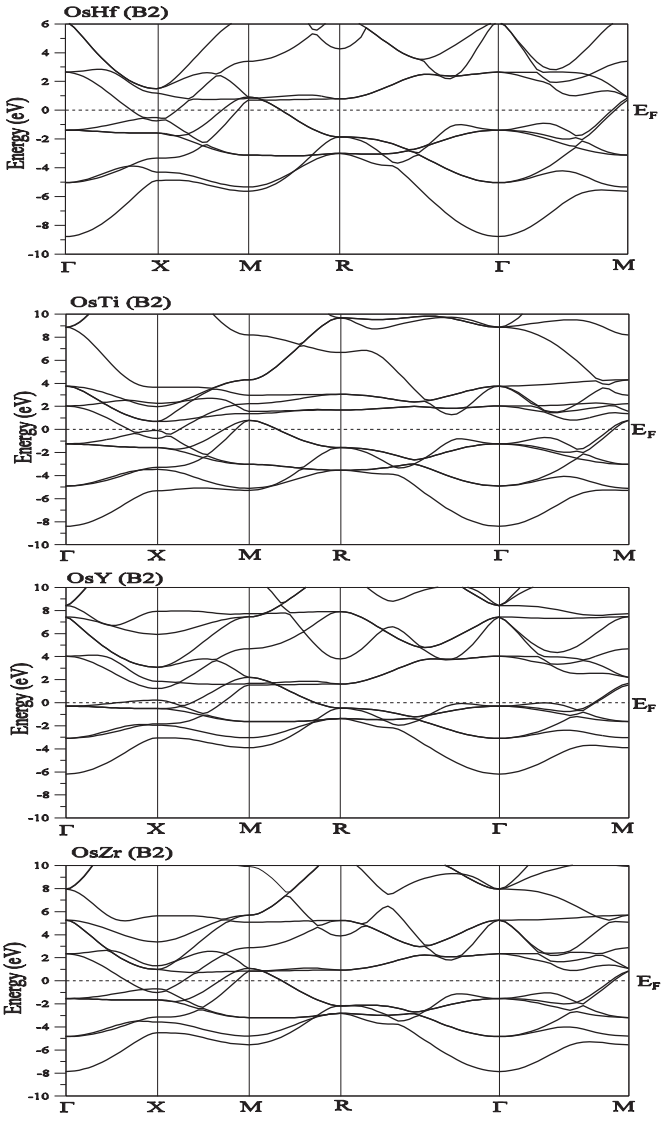

Fig. 2. The electronic band structure for OsM (M=Hf, Ti, Y and Zr) in the B2 phase.

The phonon dispersion curves and the total and partial density of states of OsM (M=Hf, Ti, Y and Zr) compounds were presented in Fig. 4. The phonon spectra of OsM (M=Hf, Ti, Y and Zr) compounds indicate that these materials are dynamically stable because phonon frequencies along all directions are positive.

The optical and acoustic phonon modes for OsHf overlapped as seen in the phonon spectra and its density of states. The mass ratios of Os and Hf are responsible for the overlap between the acoustic and optical branches of OsHf. The optical and acoustic modes of OsTi are separated from each other; it could be seen from all phonon curves and density of states. This gap was computed to be 0.607 THz. The partial density of states of OsTi, OsY, and OsZr shows that the density of states is contributed by Os atoms at low frequency region and Ti (Y and Zr) atoms at high frequency region. The optical mode frequencies at the zone center point for OsX (M=Hf, Ti, Y and Zr) are 4.582, 6.950, 5.141, and 5.657 THz, respectively. General trends of OsTi and OsY phonon dispersion curves are consistent with our earlier work on IrSc and ScPd [37,38].

Phonon density of states is plotted, and the information of lattice vibrational contribution of each atom can be obtained in

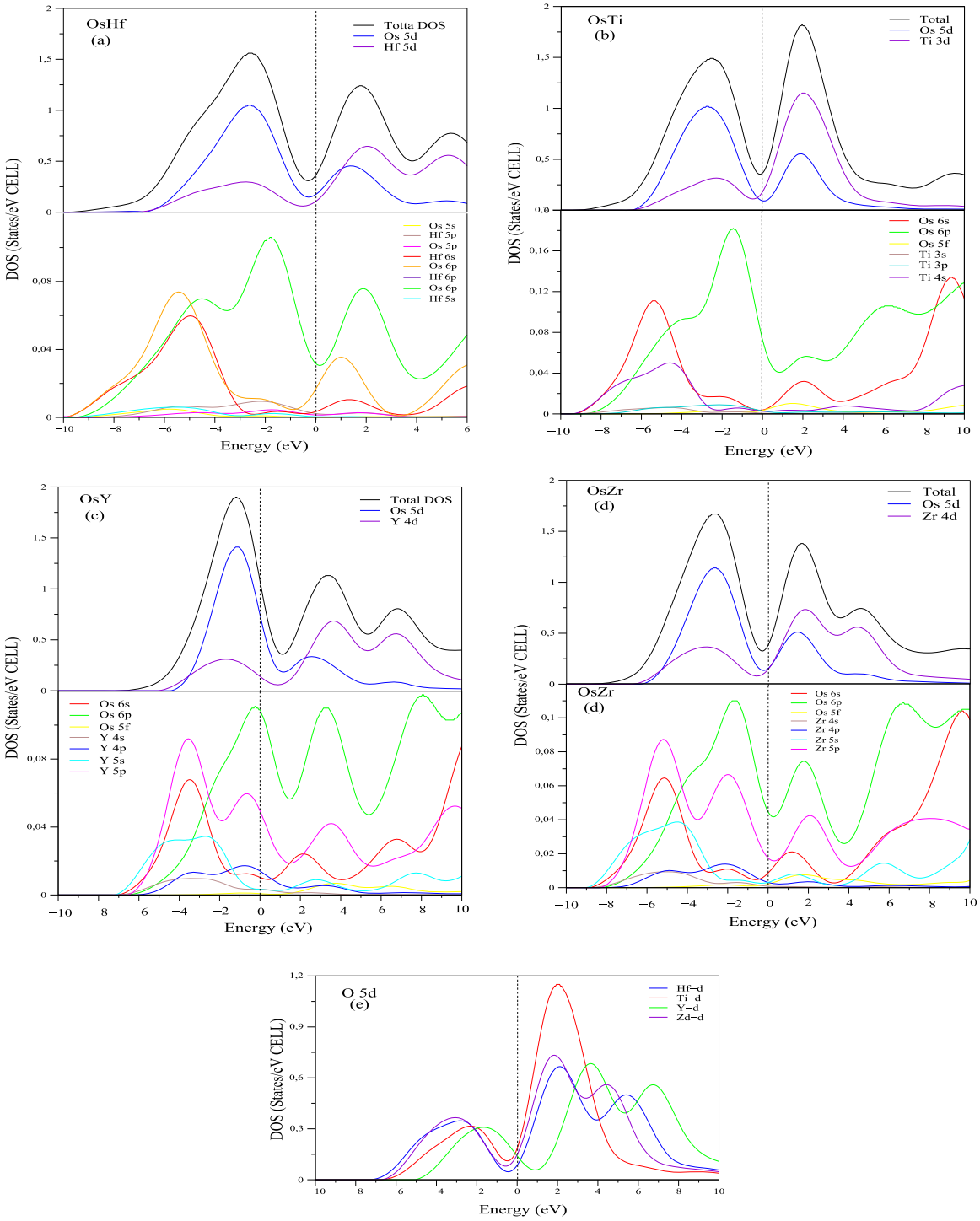

Fig. 3. The partial and total DOS for OsM (M=Hf, Ti, Y and Zr) in the B2 phase.

Fig. 4. Osmium element vibrates with small frequency that it dominates the low frequency region of partial density of states (PDOS) while Zr, Ti, and Y, relatively lighter elements, contributes to the higher frequency of movement in OsZr, OsTi, and OsY compounds. However, in OsHf, both atoms vibrate simultaneously with the same frequency spanning through the whole region of PDOS.

The calculated specific heat C_v, of OsM (M=Hf, Ti, Y and Zr) compounds as function of temperature is plotted in Fig. 5. The rapid rise of the specific heat is clearly seen, and when the temperature reaches at about 800 K, C_v becomes constant following the Dulong–Petit law. Unfortunately, no available theoretical data are available regarding the specific heat capacity of OsM (M=Hf, Ti, Y and Zr) compounds. No effect is shown on C_v by exchanging Hf by Ti, Y, or Zr atoms in OsM compounds at high temperature.

4. Conclusion

Through the first-principles functional calculations, the structural parameters and electronic and vibrational properties of OsM (M=Hf, Ti, Y and Zr) compounds were investigated. The exchange-

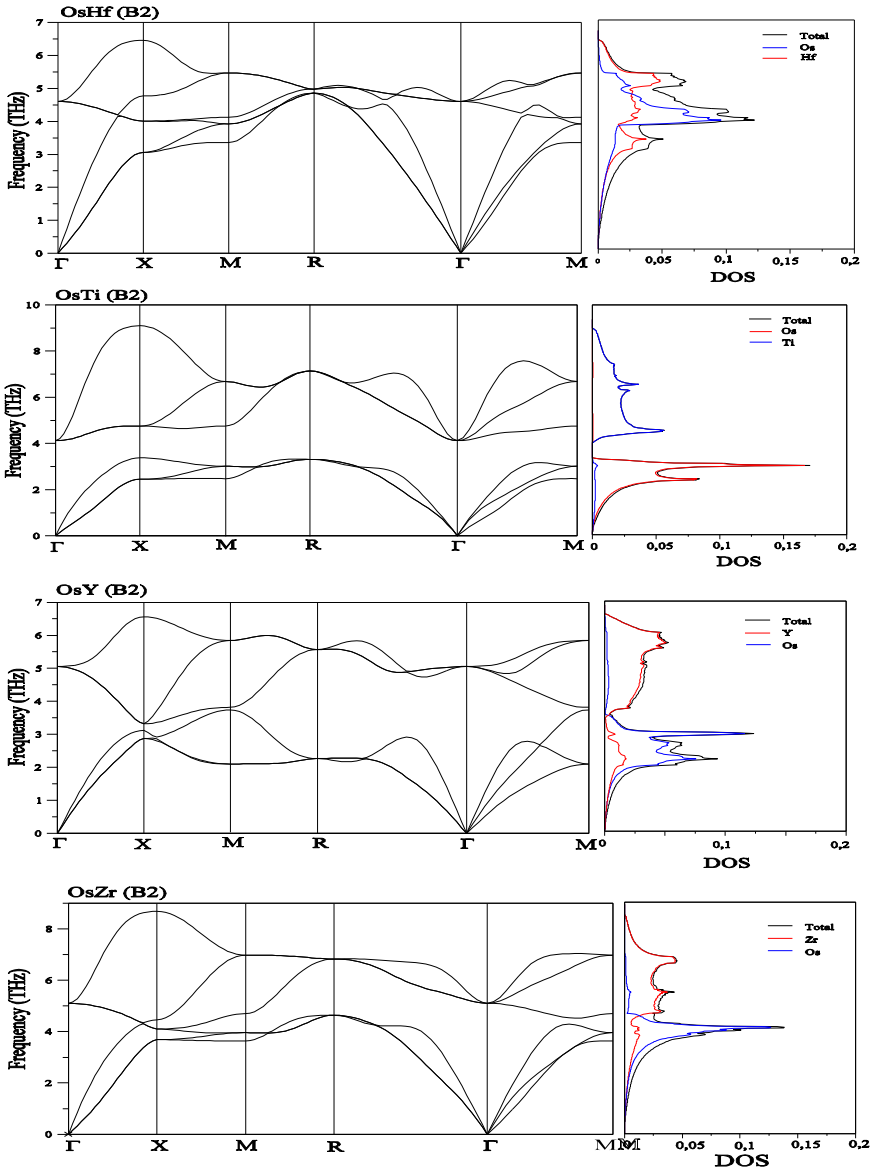

Fig. 4. The phonon dispersion curves and phonon DOS for OsM (M=Hf, Ti, Y and Zr) in the B2 phase along several lines of high symmetry in the Brillouin zone.

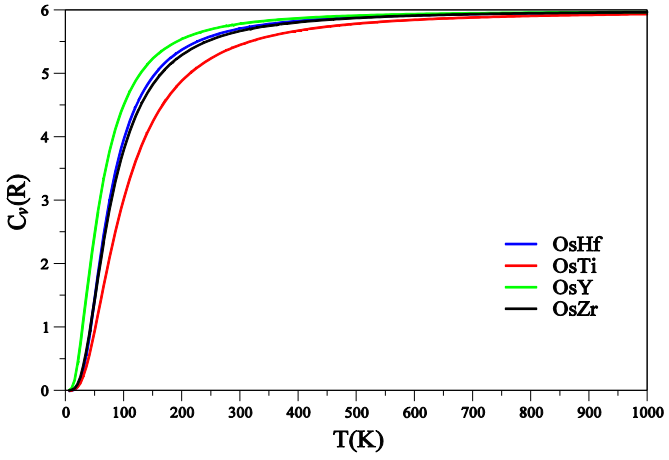

Fig. 5. The specific heats at constant volume versus temperature for OsM (M=Hf, Ti, Y and Zr) compounds.

correlation potential is treated using the generalized gradient approximation. The main focus of the present work is to study the structural, electronic, elastic, and phonon properties of OsM (M=Hf, Ti, Y and Zr) compounds and to see the effect of M atoms on the properties of OsM (M=Hf, Ti, Y and Zr) compounds.

The lattice constants were determined and are in excellent agreement with the available experimental data. It is interesting to note that the lattice parameter decreases when we move from OsHf to OsTi, and from OsY to OsZr, while the bulk modulus increases. The electronic structure for the four alloys was analysed and compared. Furthermore, the position of the Fermi level is discussed.

The elastic constants and phonon spectra of OsM (M=Hf, Ti, Y and Zr) verify their mechanical and dynamical stabilities.

All Os based compounds are weak metals with increasing metallicity as the Hf atom is replaced Ti, Zr, Y atom, in an increasing order. We found significant covalency in all these weak metallic compounds. The calculated *B/G* ratio suggests that OsHf, OsTi, OsY, and OsZr are ductile materials. The phonon density of states and phonon frequencies in the B2 phase along the high symmetry lines of the Brillouin zone were obtained and discussed

using the density-functional perturbation theory. Finally, the specific heat capacity C_v of OsM (M = Hf, Ti, Y and Zr) compounds is calculated and discussed.

References

[1] R.A. Hein, J.E. Cox, R.D. Blaugher, R.M. Waterstrat, Solid State Commun. 7 (1969) 381.
[2] O. Rapp, J. Invarsson, T. Claeson, Phys. Lett. 50A (1974) 159.
[3] R. Jerlerud-Perez, B. Sundman, CALPHAD 27 (2003) 253.
[4] S.W. Cho, C.S. Han, C.N. Park, E. Akiba, J. Alloy. Compd. 289 (1999) 244.
[5] L.D. Zardiackas (Ed.), Titanium, Niobium, Zirconium and Tantalum for Medical and Surgical Applications, ASTM International, 2006.
[6] K. Mahdouk, J. Gachon, J. Alloy. Compd. 278 (1998) 185.
[7] W. Xing, X.-Q. Chen, D. Li, Y. Li, C.L. Fu, S.V. Meschel, X. Ding, Intermetallics 28 (2012) 16.
[8] B.N. Eremenko, E.L. Semenova, T.D. Shtepa, Dokl Akad, Nauk. SSSR Ser. A 7 (1978) 661.
[9] B.N. Eremenko, E.L. Semenova, T.D. Shtepa, Izv Akad, Nauk. SSSR Met. 2 (1978) 200.
[10] N.I. Taluts, A.V. Dobromyslov, J. Alloy. Compd. 298 (2000) 181.
[11] Q.-J. Liu, Ning-Chao Zhang, Fu-Sheng Liu, Zheng-Tang Liu, J. Alloy. Compd. 589 (2014) 278.
[12] S.V. Meschel, X.Q. Chen, O.J. Kleppa, Philip Nash, CALPHAD 33 (2009) 55.
[13] C. Guo, Z. Du, J. Alloy. Compd. 407 (2006) 188.
[14] P. Giannozzi, S. Baroni, N. Bonini, M. Calandra, R. Car, C. Cavazzoni, et al., J. Phys. Condens. Matter 21 (2009) 395502 ⟨http://www.quantum-espresso.org/pseudopotentials/#⟩.
[15] E. Isaev. QHA: calculation of thermodynamic properties using the Quasi-Harmonic approximation. ⟨http://qha.qe-forge.org⟩, 2009 (accessed 22.07.13).
[16] V.N. Eremenko, T.D. Shtepa, E.L. Semenova, Russian Metallurgy, Translated from Izvestiya Akademii Nauk SSSR, Metally, vol. 4, 1971, pp. 147e149.
[17] K. Mahdouk, B. Sundman, J. Gachon, J. Alloy. Compd. 241 (1996) 199.
[18] J.E. Saal, S. Kirklin, M. Aykol, B. Meredig, C. Wolverton, Materials design and discovery with high-throughput density functional theory: the open quantum materials database (OQMD), JOM 65 (2013) 1501.
[19] J.P. Perdew, K. Burke, M. Ernzerhof, Phys. Rev. Lett. 78 (1996) 1396.
[20] K.F. Garrity, J.W. Bennett, K.M. Rabe, D. Vanderbilt, Comput. Mater. Sci. 81 (2014) 446.
[21] H.J. Monkhorst, J.D. Pack, Phys. Rev. B 13 (1972) 5188.
[22] M. Methfessel, A.T. Paxton, Phys. Rev. B 40 (1989) 3616.
[23] S. Baroni, P. Giannozzi, A. Testa, Phys. Rev. Lett. 58 (1987) 1861.
[24] M.E. Fine, L.D. Brown, H.L. Marcus, Src. Metall. 18 (1984) 951.
[25] S.Q. Wang, H.Q. Ye, Phys. Stat. Solidi (b) 240 (2003) 45.
[26] A. Erba, M. Shahrokhi, R. Moradian, R. Dovesi, J. Chem. Phys. 142 (2015) 044114.
[27] F.D. Murnaghan, Proc. Nat. Acad. Sci. USA 30 (1944) 244.
[28] A.E. Dwight, Trans. Metall. Soc. AIME 215 (1959) 283.
[29] V.N. Eremenko, T.D. Shtepa, E.L. Semenova, The Ti–Os phase diagram, Izv. Akad. Nauk. SSSR Met. (2) (1971) 210–213, in Russian.
[30] K. Takemura, Phys. Rev. B 70 (2004) 012101.
[31] F. Occelli, D.L. Farber, J. Badro, C.M. Aracne, D.M. Teter, M. Hanfland, B. Canny, B. Couzinet, Phys. Rev. Lett. 93 (2004) 095502.
[32] M. Born, K. Huang, Dynamical Theory of Crystal Lattices, Clarendon, Oxford, 1954.
[33] S.F. Pugh, Philos. Mag. 45 (1954) 823.
[34] Ş. Uğur, A. İyigör, Z. Charifi, H. Baaziz, M.R. Ellialtıoğlu, Philos. Mag. 93 (2013) 3260.
[35] R. Eiblert, A. Neckelt, J. Phys. F: Met. Phys. 10 (1980) 2179.
[36] M. Krčmar, C.L. Fu, Phys. Rev. B 68 (2003) 134110.
[37] N. Arıkan, Z. Charifi, H. Baaziz, Ş. Uğur, H. Ünver, G. Uğur, J. Phys. Chem. Solids 77 (2015) 126.
[38] N. Arıkan, Ş. Uğur, Comput. Mater. Sci. 47 (2010) 668.